

Sedimentologic and geomorphic evidence for seesaw subsidence of the Santo Domingo accommodation-zone basin, Rio Grande rift, New Mexico

Gary A. Smith*

Department of Earth and Planetary Sciences, University of New Mexico, Albuquerque, New Mexico 87131, USA

William McIntosh

New Mexico Bureau of Mines and Mineral Resources, New Mexico Institute of Mines and Technology, Socorro, New Mexico 87801, USA

Andrika J. Kuhle†

Department of Earth and Planetary Sciences, University of New Mexico, Albuquerque, New Mexico 87131, USA

ABSTRACT

Basin analysis of facies patterns and basin geomorphology reveals a complex subsidence pattern for part of the Rio Grande rift in north-central New Mexico, United States. The Santo Domingo basin study site is located in the accommodation zone between the east-tilted northern Albuquerque basin and the west-tilted Española basin half-graben. Upper Miocene through lower Pleistocene basin-fill sediment records a longitudinal, south-flowing, ancestral Rio Grande and flanking piedmont stream systems. Chronology of deposition is provided by $^{40}\text{Ar}/^{39}\text{Ar}$ geochronological study of lava flows and pyroclastic deposits interbedded with the sediment. Down-to-the-east faults concentrated in the western basin illustrate increasing displacement toward the north and merge with structures forming the western margin of the Española basin. Down-to-the-west faults in the central and eastern basin exhibit southward-increasing displacement and become the principal structures along the eastern margin of the northern Albuquerque basin. The latitudinal overlap of these fault systems in the Santo Domingo basin gives the appearance of a symmetrical graben with anticlinal bedding attitudes. Analysis of the distribution of sedimentary facies, high-level geomorphic surfaces, and Pleistocene terraces indicates, however, that the basin subsided

in a seesaw fashion rather than as a symmetrical graben. During the late Miocene and early Pliocene, the course of the ancestral Rio Grande was deflected to the west, suggesting strong westward tilting of the basin. In late Pliocene and Pleistocene time, however, eastward tilting brought the river into the eastern basin. At that time, an east-sloping pediment was eroded across west-dipping strata in the western basin. Pediment gravel and tuff present as unconformity-bounded strata in the western basin correlate with continuously aggraded conformable basin-fill strata to the east. A return to westward tilting since middle Pleistocene time is suggested by unpaired terraces consistent with net westward migration of the Rio Grande, lack of post-middle Pleistocene motion on faults in the eastern basin, and numerous fault displacements of the pediment gravel in the western basin.

Keywords: accommodation zone, basin subsidence, rift basin, Rio Grande rift, Santo Domingo basin.

INTRODUCTION

Most extensional basins are asymmetric graben or half-graben that subsided with a virtually unidirectional tilt, which is reflected both in the development of predominant structural relief along one basin margin and in the asymmetric pattern of sedimentary facies within the basin (e.g., Leeder and Gawthorpe, 1987). The longitudinal river in hydrologically open basins will

likely be displaced toward the more strongly downtilted side of the basin, as suggested by numerical models (Bridge and Leeder, 1981; Bridge and Mackay, 1993) and as is consistent with field observations (Mack and Seager, 1990; Alexander et al., 1994; Blair and McPherson, 1994; Leeder et al., 1996; Peakall, 1998).

Although symmetrical-appearing graben are common in accommodation zones (Rosendahl, 1987; Morley et al., 1990; Faulds and Varga, 1998), sedimentation patterns within them are less well known. Such graben actually are facing half-graben, and there is no compelling reason why strain rates should be equal in both master-fault systems. Rosendahl (1987) suggested that simultaneous subsidence of both master faults is mechanically difficult. Rosendahl (1987) interpreted seismic-reflection lines across East African rift valley lakes as indicating that such basins subside in a seesaw fashion.

The purpose of this paper is to demonstrate utility of sedimentological and geomorphological analyses to interpret the subsidence history of an accommodation-zone basin. Specifically, we document a complicated seesaw subsidence history of alternate-direction tilting for the Santo Domingo basin within the Rio Grande rift of north-central New Mexico. The interpretation is based on integration of sedimentological and geomorphic observations including sedimentary facies patterns, development of fluvial erosion surfaces, and preservation of fluvial terraces coupled with geologic mapping and $^{40}\text{Ar}/^{39}\text{Ar}$ geochronology of associated volcanic deposits. The approach may be useful for unraveling subsi-

*E-mail: gsmith@unm.edu.

†Present address: Land and Water Consulting, P.O. Box 8027, Kalispell, Montana 59901, USA.

dence patterns in other extensional basins where, like the Santo Domingo basin, there are no pertinent subsurface well or seismic-reflection data.

STUDY SITE

The Rio Grande rift is a narrow zone within the broader region of Neogene extension in the western United States that trends north-south through central New Mexico (Fig. 1). Initial subsidence began in Oligocene or early Miocene time in most rift basins (Chapin and Cather, 1994). Although some adjacent basins were hydrologically linked through most or all of their development, the establishment of the through-flowing Rio Grande along the length of the rift was not completed until Pleistocene time. Most basins are half-graben or strongly asymmetric graben. Accommodation zones include both transfer structures, at a high angle to the rift trend, and strike-parallel antithetic zones (Faults and Varga, 1998) of latitudinal overlap of master faults that bound adjacent basins of opposite tilt polarity. The structure and stratigraphic architecture of the Santo Domingo basin presented in this paper result primarily from recent 1:24 000 scale geologic mapping (Smith and Kuhle, 1998a, 1998b; Chamberlin et al., 1999; unpublished mapping by G. Smith and A. Kuhle, 1994–1997; Figs. 2, 3, and 4) and complementary geochronological study of volcanic materials within the basin fill.

The Santo Domingo basin is astride the transition from the east-tilted northern Albuquerque basin to the west-tilted Española basin half-graben and has been treated as a part of (e.g., Kelley, 1977), or structurally distinct from (e.g., Lozinsky, 1994), the northern Albuquerque basin (Fig. 1). The structural margins of the basin probably varied through time. For the purpose of this discussion we focus on the basin as defined by faults constraining the distribution of thick, post-7 Ma basin fill. Therefore, we define its boundaries as the Santa Ana fault, on the west, continuing as far east as the La Bajada fault. To the south of our study area the eastern rift boundary steps westward across relay ramps so that the San Francisco fault also forms part of the Santo Domingo basin boundary (Fig. 1). The Santa Ana fault is chosen as the boundary of the Santo Domingo basin because: (1) it represents the westernmost of a series of down-to-the-east faults that separate largely middle Miocene and older strata, on the west, from younger basin fill on the east; (2) these faults continue northward into the Jemez Mountains volcanic field (Cañada de Cochiti fault zone of Gardner et al., 1986), where they closely approximate the rift margin; and (3) these

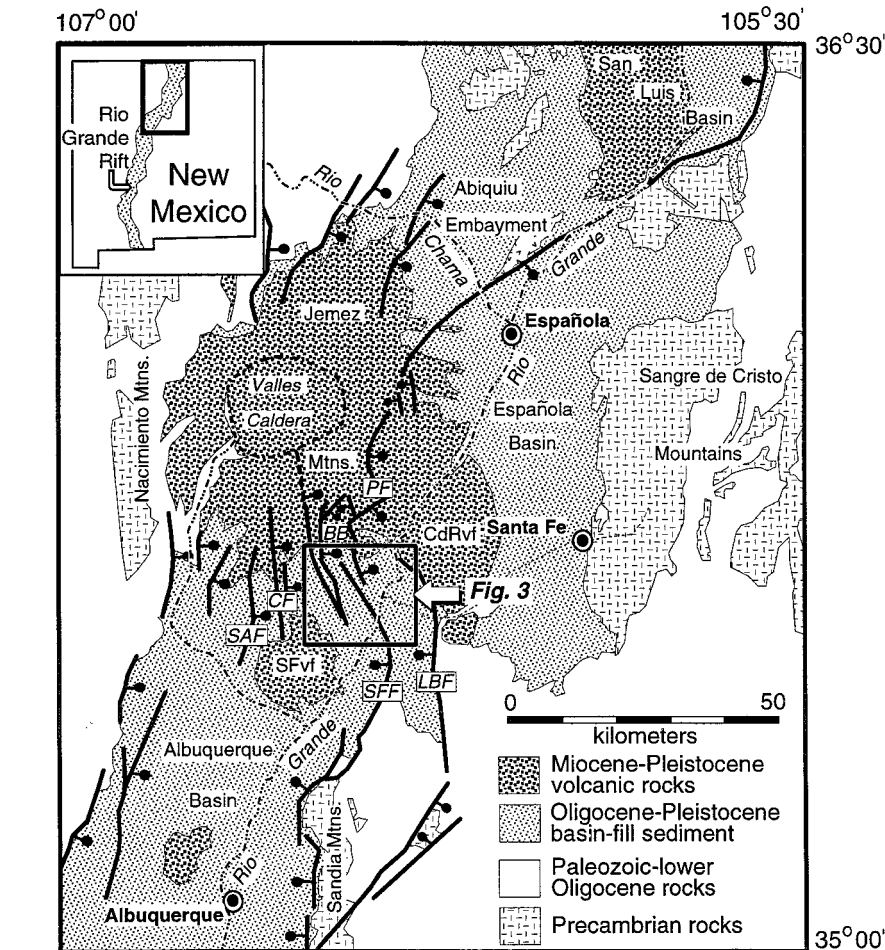


Figure 1. Index map of the Rio Grande rift in northern New Mexico showing principal faults, volcanic features, and basins discussed in the text. CF—Cocida fault, LBF—La Bajada fault, PF—Pajarito fault, SAF—Santa Ana fault, SFF—San Francisco fault, BB—Bearhead basin, CdRvf—Cerros del Rio volcanic field, SFvf—San Felipe volcanic field.

faults correspond closely with the sharply defined edge of the 20 mgal isostatic residual gravity anomaly that geophysically defines the Santo Domingo basin (Heywood, 1992). Principal late Miocene and younger subsidence was, however, focused along and east of the Cocida fault (see following). The northern and southern boundaries are arbitrary because the basin is not structurally isolated from the Albuquerque or Española basins. Gravity data (Heywood, 1992; Grauch et al., 1999) suggest that a structural bench, opposite the northern Sandia Mountains, separates the Albuquerque and Santo Domingo basin depocenters. The Jemez Mountains and Cerros del Rio volcanic fields form a prominent topographic, and partly structural, boundary along most of the northern part of the basin.

GEOCHRONOLOGY

We analyzed 16 samples by the $^{40}\text{Ar}/^{39}\text{Ar}$ method at the New Mexico Geochronology

Research Laboratory. Sanidine crystals were separated from nine primary or reworked rhyolitic tephra layers, and groundmass concentrates were prepared from six basaltic lava flows (Table 1). After irradiation, sanidine crystals were analyzed following CO_2 laser fusion. With two exceptions crystals were sufficiently large for single-crystal laser fusion; aliquots of two to five small crystals were fused for the two finest grained samples (Table 2). Basaltic groundmass was analyzed by the resistance-furnace incremental heating method. Separation and analytical methods are detailed in Table 2 and in McIntosh and Chamberlin (1994); (data are presented in Tables DR1 and DR2 in the GSA Data Repository)¹.

¹GSA Data Repository item 2001039, Analytical data, is available on the Web at <http://www.geosociety.org/pubs/ft2001.htm>. Requests may also be sent to Documents Secretary, GSA, P.O. Box 9140, Boulder, CO 80301; e-mail: editing@geosociety.org.

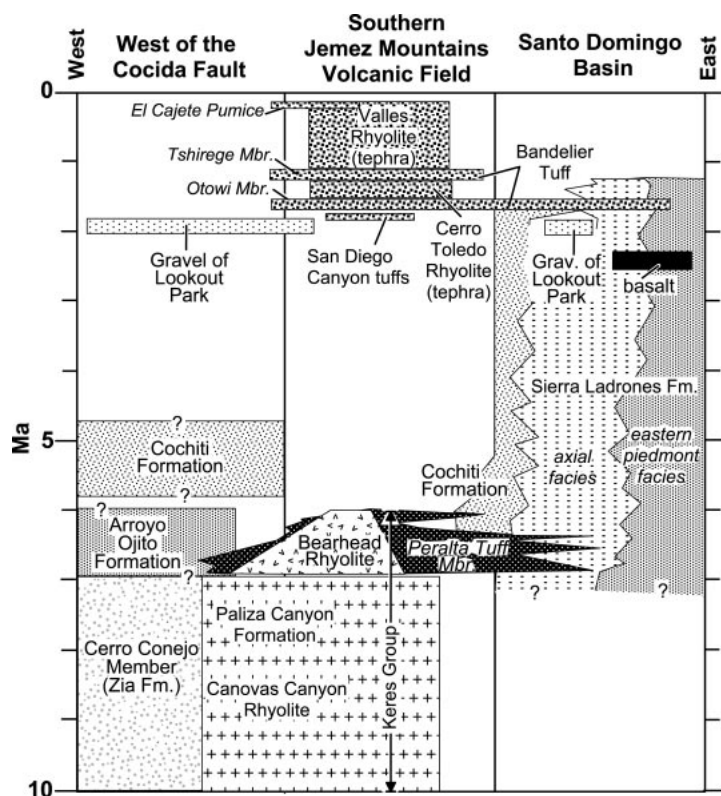


Figure 2. Generalized chronostratigraphy of late Cenozoic strata in and near the Santo Domingo basin showing relationships between Santa Fe Group sedimentary basin fill and volcanic rocks of the Jemez Mountains volcanic field.

Most individual laser-fusion age determinations for the nine sanidine separates form single, tightly grouped, near-Gaussian age populations (Fig. 5). Of the 113 crystals analyzed, only 9 have anomalous ages; 3 of these are significantly older than the near-Gaussian age populations, and are interpreted as xenocrystic or detrital contaminants (Table DR1; see text footnote 1). Six crystals (denoted by open symbols in Fig. 5) have slightly anomalous ages, possibly due to minor alteration or incomplete removal of surficial glass. After excluding these data from these nine crystals, weighted mean ages for the nine samples range from 0.55 to 6.84 Ma, with $+2\sigma$ errors between ± 0.02 and ± 0.07 Ma. Variations in these weighted mean errors, and in the precision and scatter of individual fusion ages, are largely a function of crystal size and the number of laser-fusion analyses performed. The errors in the $^{40}\text{Ar}/^{39}\text{Ar}$ age determinations are sufficiently small to allow relatively confident correlations with previously dated volcanic deposits, principally originating from the Jemez Mountains.

Basaltic-groundmass concentrates provided high radiogenic yields, with one exception (sample GSSSD367), and apparent ages of in-

dividual steps are precise (Fig. 6). The low radiogenic yields and consequent low precision of the age spectrum of sample GSSD367 (Fig. 6E) probably reflect large amounts of groundmass glass. Three of the six age spectra (Fig. 6, A, E, and F) are nearly flat; most or all of the heating steps satisfy plateau criteria (Table 2; Fig. 6). The remaining three spectra (Fig. 6, B, C, and D; from well cuttings) decline slightly from low to high temperatures, possibly reflecting minor recoil redistribution of ^{39}Ar or alteration of groundmass glass. Central parts of these declining spectra satisfy plateau criteria and define plateau ages (Fig. 6; Table 2; Table DR2 [see text footnote 1]). The plateau ages for these three cannot be resolved at the $\pm 2\sigma$ level, particularly given the slightly disturbed nature of their age spectra.

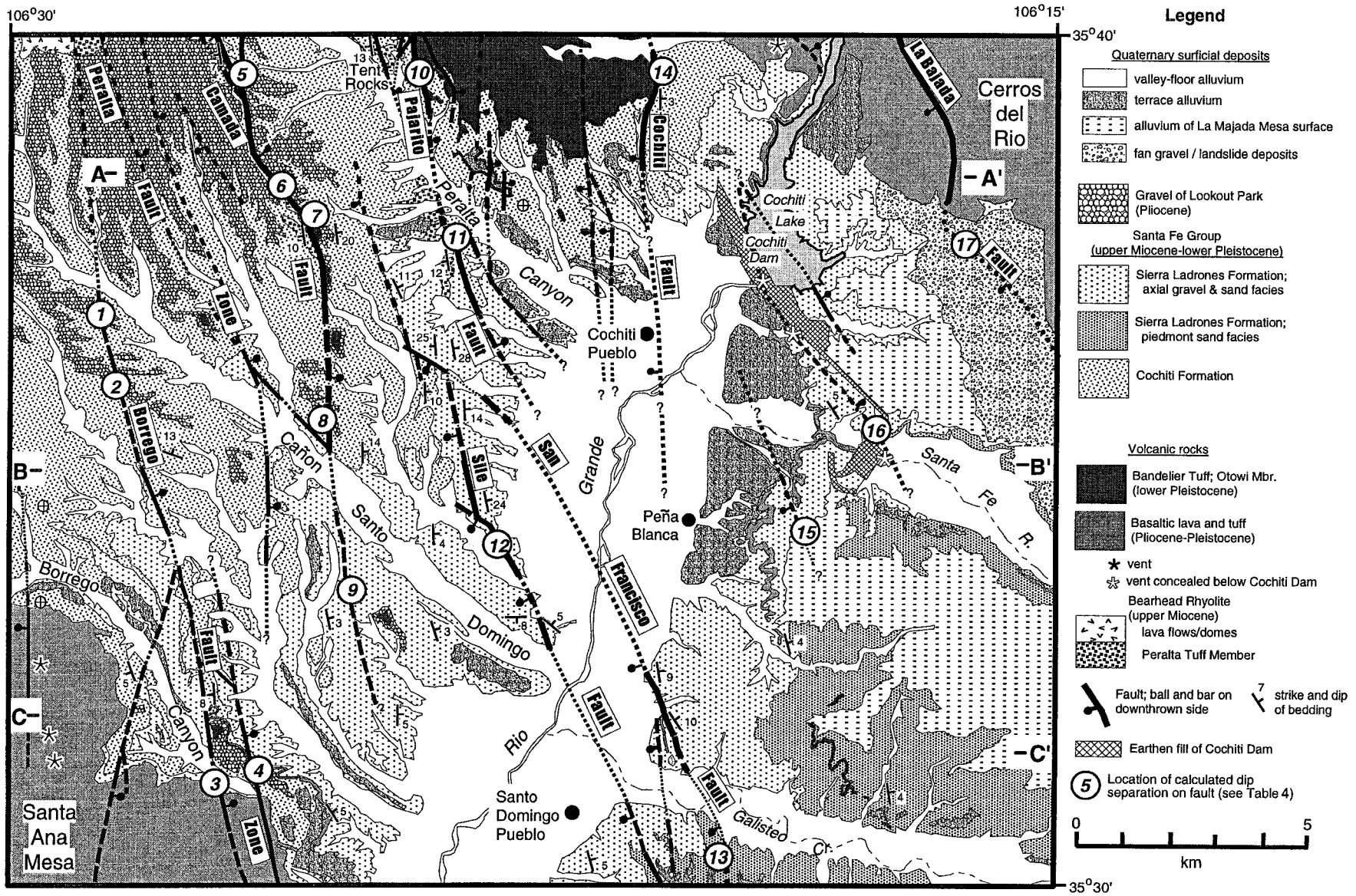
Plateau ages for the six groundmass concentrates range from 2.41 to 2.71 Ma, with $\pm 2\sigma$ errors ranging from ± 0.02 to ± 0.06 Ma, except for sample GSSD367 (Fig. 6E), which has a 2σ error of ± 0.15 Ma. For each of the six samples there is close agreement among plateau, isochron (Table 2), and integrated ages (Fig. 6). The high MSWD (mean square of weighted deviations) values for the isochrons of some of the samples reflect high analytical precision coupled

with minor disturbances of the age spectra described here. None of the isochrons have $^{40}\text{Ar}/^{36}\text{Ar}$ intercepts indicative of significant excess ^{40}Ar (Table 2). A probability-distribution diagram underscores the generally close agreement among the plateau ages of the six basaltic groundmass samples; only the age of the youngest sample (GSSD311 in Fig. 5C) is distinct at the $\pm 2\sigma$ level.

BASIN-FILL STRATIGRAPHY

Sedimentary fill of Rio Grande rift basins is broadly assigned to the Santa Fe Group (Fig. 2). Regionally, these strata accumulated between Oligocene or early Miocene time and Pliocene–Pleistocene base-level fall and incision of the Rio Grande and its principal tributaries. Most sedimentary strata within the Santo Domingo basin are assigned to the upper Miocene–lower Pleistocene Sierra Ladrones and Cochiti Formations, which are described further in the following. Partly correlative strata of the Arroyo Ojito Formation (Connell et al., 1999) and the older middle Miocene Cerro Conejo Member of the Zia Formation (Connell et al., 1999) crop out along the western margin between the Santa Ana and Cocida faults. Both the Arroyo Ojito Formation and Cerro Conejo Member in the footwall of the Cocida fault consist mostly of fluvial facies reflecting intercalation of coarse-grained volcanoclastic debris, shed southward from the Jemez Mountains, and a generally upward-coarsening assemblage of arkosic and quartzo-lithic sandstone and conglomeratic sandstone that document streams flowing eastward from the Nacimiento Mountains.

Volcanic rocks are intimately interbedded with the Santa Fe Group near the basin margins (Fig. 2). Most voluminous are the middle Miocene to Pleistocene lava flows, domes, and tuffs composing the Jemez Mountains volcanic field (Gardner et al., 1986). Jemez volcanic rocks are principally found north of the study area but were also erupted along the western basin margin. Of particular importance is the upper Miocene Bearhead Rhyolite, including pyroclastic and sedimentary deposits of the Peralta Tuff Member (Fig. 2). The Otowi Member of the Bandelier Tuff is found discontinuously through most of the mapped area (Fig. 3). Pliocene, mostly basaltic, lava flows of the San Felipe (Santa Ana Mesa) and Cerros del Rio volcanic fields are present along the southwestern and northeastern basin margins, respectively. Correlative basalt was erupted within the eastern basin from vents largely concealed beneath Cochiti Dam (Fig. 3; Smith et al., 1997). Temporal patterns of sedimentation have been reconstructed



SMITH et al.

Figure 3. Geologic map of the central Santo Domingo basin (after Smith and Kuhle, 1998c). Note locations of cross sections depicted in Figure 4.

TABLE 1. SUMMARY OF $^{40}\text{Ar}/^{39}\text{Ar}$ AGE DETERMINATIONS FOR SAMPLES IN THE SANTO DOMINGO BASIN

Sample number	Field number	Sample description	Location (UTM)	Age (Ma)
Sanidine, laser-fusion analyses				
1	GSCP9612	Reworked crystal rich biotite-rhyolite ash forming matrix to flood deposit in Qt_2 terrace fill on west side of Cochiti Lake; correlative with Valles Rhyolite	80694542	0.55 ± 0.01
2	GSCP9605	Reworked rhyolitic pumiceous ash collected within axial quartzite-rich gravel just east of the south abutment of Cochiti Dam; probably reworked Otowi Member, Bandelier Tuff.	82923760	1.62 ± 0.01
3	GSCP9611	Reworked rhyolitic pumice-fall deposit; roadcut west of Cochiti Lake	78244676	1.84 ± 0.01
4	GSCP9610	Rhyolitic pumice-fall deposit with distinctive "soda-straw" vesicles in lapilli as characteristic of ejecta from San Diego Canyon ignimbrite A; roadcut west of Cochiti Lake	78244676	1.87 ± 0.01
5	GSTR9701	Rhyolitic pumice-fall deposit within lower part of Cochiti Fm. at Tent Rocks	72754708	6.19 ± 0.06
6	GSCP9601	Rhyolitic pumice, reworked; within axial gravel of the Sierra Ladrones Fm. Near Sile fault west of Peña Blanca; correlative to pyroclastic deposits in Peralta Tuff.	74453744	6.82 ± 0.04
7	GSCP9603	Rhyolitic pumice-fall deposit within axial gravel of the Sierra Ladrones Fm. west of Cochiti Pueblo; correlative to pyroclastic deposits in Peralta Tuff Member of the Bearhead Rhyolite.	73924242	6.88 ± 0.01
8	GSCP9615	Rhyolitic pumice-fall deposit, Peralta Tuff Member of the Bearhead Rhyolite in area southwest of Peralta Canyon where Peralta Tuff is interbedded with axial gravel of the Sierra Ladrones Fm.	73564277	6.81 ± 0.02
9	GSCP9623	Rhyolitic ignimbrite pumice, Peralta Tuff Member of the Bearhead Rhyolite south of Peralta Canyon	70704304	6.84 ± 0.06
Plateau ages, incremental step heating of groundmass separates				
10	DN9615	Lower of two basalt flows interbedded with Sierra Ladrones Fm. near Cochiti Spring in the Santa Fe River valley downstream of Cochiti Dam (collected by D.P. Dethier)	82003848	2.71 ± 0.04
11	SCST640-650	Olivine-basalt lava flow; sample collected from cuttings at 195-198 m in the Bureau of Indian Affairs Santa Cruz Springs Tract well	86523908	2.67 ± 0.06
12	SCST720-730	Hawaiite lava flow; sample collected from cuttings at 219-222 m in the Bureau of Indian Affairs Santa Cruz Springs Tract well	86523908	2.57 ± 0.03
13	SCST850-860	Hawaiite lava flow; sample collected from cuttings at 259-262 m in the Bureau of Indian Affairs Santa Cruz Springs Tract well	86523908	2.57 ± 0.02
14	GSSD367	Olivine basalt; thin flow intercalated within near-vent agglutinate on Santa Ana Mesa	64943174	2.62 ± 0.15
15	GSSD311	Olivine basalt lava flow overlying hydromagmatic tuff north of Borrego Canyon; downfaulted equivalent of lava flow forming northern rim of Santa Ana Mesa.	70863049	2.41 ± 0.03

through geochronological study of these associated volcanic rocks (Table 1).

Sierra Ladrones Formation

Upper Miocene through Quaternary sediment between the Cocida and La Bajada faults can be attributed to deposition by a southward-flowing axial river (ancestral Rio Grande) and by southwestward- and southeastward-flowing streams on flanking piedmonts. Axial-river and eastern-piedmont facies are assigned to the Sierra Ladrones Formation. The base of the Sierra Ladrones Formation is not exposed, but at least 350 m of continuous dipping section is mapped in the central and eastern part of the basin (Fig. 4).

Axial-river deposits consist of unconsolidated to slightly cemented gravel and sand, interbedded with lenticular tuffaceous mud. The prominence of clasts, most notably quartzite, derived from extrabasinal sources in northern New Mexico (Smith and Kuhle, 1998c) demonstrates deposition along the course of a south-flowing river.

The exposed eastern-piedmont facies of the Sierra Ladrones Formation is fine sand and silt with ~10%–20% sandy, pebble to cobble gravel. It is likely that coarser grained basin-margin facies are concealed in the subsurface of the eastern part of the mapped area. Gravel clasts indicate sources east and northeast of the basin and delivery of sediment by streams analogous to the modern Santa Fe River and Galisteo Creek (Smith and Kuhle, 1998a). The eastern-

piedmont deposits are intimately interbedded with the axial facies east of the present Rio Grande.

Axial-river gravel is interlayered with the Peralta Tuff Member of the Bearhead Rhyolite along the south side of Peralta Canyon (Fig. 3). Pyroclastic deposits intercalated in quartzite-rich gravel are 6.81–6.88 Ma (Table 1, samples 6–9). Hydrovolcanic eruptions at 6.96 Ma (Smith et al., 1991; McIntosh and Quade, 1995) from a rhyolite vent 2.4 km northwest of Tent Rocks (Fig. 3) expelled axial-composition clasts and large (to 6 m) blocks of axial facies sediment (Smith et al., 1991; Gay and Smith, 1996).

These relationships indicate an antiquity of at least 7 Ma for axial-river gravel in the Santo Domingo basin, the base of which is nowhere exposed, in contrast to previous perceptions (e.g., Lozinsky, 1994) that a gravel-bedload river did not enter the Albuquerque basin from the north until after 5 Ma. The lower part of the axial-river facies may be correlative with the informal Chaquhui formation of Purtymun (1995), which is known only in the subsurface west of the Rio Grande in the Española basin and is associated with volcanic rocks as old as 8–9 Ma. We do not know of deposits with comparable texture and composition in upper Miocene strata north or northeast of Española. However, clasts found in the Santo Domingo basin (quartzite, metavolcanic rocks, granite, and distinctive Miocene chert and welded tuff) are found within the watershed of the modern Rio Chama (Fig. 1). We there-

fore suggest that the Miocene axial river was more closely associated with the Rio Chama watershed than the modern Rio Grande north of Española.

The 1.61 Ma Otowi Member of the Bandelier Tuff is present within the eastern piedmont facies north of Galisteo Creek. Distinctive pumice derived from either the Otowi Member (Table 1, sample 2) or the 1.22 Ma Tshirege Member is present in the axial-gravel facies, mostly east of the Rio Grande. This establishes an early Pleistocene age for the upper Sierra Ladrones Formation in the eastern Santo Domingo basin. A 2.71 Ma basalt flow (Table 1, sample 10) is also present within the formation near Peña Blanca.

Cochiti Formation

Western-piedmont gravel and sand interbedded with the Sierra Ladrones Formation are assigned to the Cochiti Formation. As revised by Smith and Lavine (1996) and Smith and Kuhle (1998c), the Cochiti Formation gradationally overlies the Peralta Tuff Member of the Bearhead Rhyolite. No single section contains both the top and bottom of the formation. A 600-m-thick section, with an eroded top, is present near Tent Rocks (Fig. 3).

The Cochiti Formation consists of cobble to boulder gravel near faults along the western basin margin and in the foothills of the Jemez Mountains and grades to a gravelly sand-dominated section where interbedded with axial gravel near the basin center. Clast composition

TABLE 2. SUMMARY OF $^{40}\text{Ar}/^{39}\text{Ar}$ RESULTS FROM SANTA DOMINGO BASIN

Sample	Laboratory numbers	Irradiation	aliquot	n	K/Ca	$\pm 2\sigma$	MSWD	$^{40}\text{Ar}/^{36}\text{Ar}$	$\pm 2\sigma$	% ^{39}Ar	Isochron		Plateau	
											Age (Ma)	$\pm 2\sigma$	Age (Ma)	$\pm 2\sigma$
Tephra: sanidine, laser-fusion														
CP-96-12	7164	NM-58	five crystals	14	56.1	4.9	N.D.	N.D.	N.D.	N.D.	N.D.	N.D.	0.55	0.02
CP-96-05	7163	NM-58	single-crystal	8	35.0	16.1	N.D.	N.D.	N.D.	N.D.	N.D.	N.D.	1.62	0.02
CP-96-11	7159	NM-58	single-crystal	12	13.0	3.1	N.D.	N.D.	N.D.	N.D.	N.D.	N.D.	1.84	0.03
CP-96-10	7162	NM-58	single-crystal	12	13.9	3.4	N.D.	N.D.	N.D.	N.D.	N.D.	N.D.	1.87	0.02
GSTR-9701	8353	NM-77	single-crystal	6	84.0	8.7	N.D.	N.D.	N.D.	N.D.	N.D.	N.D.	6.19	0.06
GSCP-96-01	7870	NM-69	single-crystal	17	50.9	23.7	N.D.	N.D.	N.D.	N.D.	N.D.	N.D.	6.83	0.05
CP-96-03	7160	NM-58	single-crystal	15	47.1	5.3	N.D.	N.D.	N.D.	N.D.	N.D.	N.D.	6.88	0.04
CP-96-15	7165	NM-58	two crystals	10	49.3	6.2	N.D.	N.D.	N.D.	N.D.	N.D.	N.D.	6.81	0.06
GSCP-96-23	7869	NM-69	single-crystal	12	39.8	27.6	N.D.	N.D.	N.D.	N.D.	N.D.	N.D.	6.84	0.07
Basaltic lava, groundmass, resistance-furnace incremental heating														
DN-96-15	6929-01	NM-54	73.3 mg	8	0.4	N.D.	2.8	295.9	3.2	99.7	2.70	0.04	2.71	0.04
SCST 640-650	7761-01	NM-65	52.9 mg	5	0.8	N.D.	25.4	290.9	7.2	77.4	2.70	0.02	2.67	0.06
SCST 720-730	7760-01	NM-65	52.1 mg	3	0.7	N.D.	3.3	294.5	9.2	49.0	2.57	0.04	2.57	0.03
SCST 850-860	7759-01	NM-65	65.6 mg	5	0.7	N.D.	1.8	295.1	2.8	68.7	2.57	0.02	2.57	0.02
GSSD-367	8958-01	NM-86	87.5 mg	5	0.2	N.D.	2.3	298.3	2.2	94.8	2.45	0.30	2.62	0.15
GSSD-311	8364-01	NM-77	64.7 mg	6	0.4	N.D.	4.0	295.0	4.0	84.0	2.41	0.02	2.41	0.03

Notes: n—number of heating steps, K/Ca—molar ratio calculated from reactor produced ^{39}Ar -K and ^{37}Ar -Ca, N.D.—not done (isochron analyses not performed on laser-fusion analyses because of high radiogenic yields). **Methods:** Sample preparation: sanidine—crushing, LST heavy liquid, Franz, HF; basaltic groundmass concentrates—crushing, picking. Irradiation: six separate in vacuo 7 h irradiations (NM-54, NM-58, NM-65, NM-69, NM-77, NM-86), D-3 position, Nuclear Science Center, College Station, Texas. Neutron flux monitor: sample FC-1 of interlaboratory standard Fish Canyon Tuff sanidine with an assigned age of 27.84 Ma (Deino and Potts, 1990), relative to Mmhb-1 at 520.4 Ma (Samson and Alexander, 1987); samples and monitors irradiated in alternating holes in machined Al disks. **Laboratory:** New Mexico Geochronology Research Laboratory, Socorro. Instrumentation: Mass Analyzer Products 215–50 mass spectrometer on-line with automated, all-metal extraction system. Heating: sanidine—single-crystal laser-fusion (SCLF), 10 W continuous CO_2 laser; vitrophyric glass—25 to 45 mg aliquots in resistance furnace. Reactive gas cleanup: SAES GP-50 getters operated at 20 °C and ~450 °C; sanidine—1 to 2 min, vitrophyric glass—9 min. Error calculation: all errors reported at $\pm 2\sigma$, mean ages calculated using inverse variance weighting of Samson and Alexander (1987), Plateau criteria: Three or more consecutive analytically equivalent ($\pm 2\sigma$) steps totaling greater than 50% of released ^{39}Ar . Decay constant and isotopic abundances: Steiger and Jaeger (1977). Complete data set: GSA Data Repository Tables DR1 and DR2. **Analytical parameters:** electron multiplier sensitivity = 1 to 3×10^{-17} moles/pA; typical system blanks were 300, 3, 1, 1, 2×10^{-18} moles (laser) and at 4800, 14, 6, 5, 18 (furnace) at masses 40, 39, 38, 37, 36, respectively; J-factors determined to a precision of $\pm 0.2\%$ using SCLF of 4 to 6 crystals from each of 4 to 6 radial positions around irradiation vessel. Correction factors for interfering nuclear reactions, determined using K-glass and CaF_2 , ($^{40}\text{Ar}/^{39}\text{Ar}$) K = 0.00020 ± 0.0003 ; ($^{36}\text{Ar}/^{37}\text{Ar}$) Ca = 0.00026 ± 0.00002 ; and ($^{39}\text{Ar}/^{37}\text{Ar}$) Ca = 0.00070 ± 0.00005 .

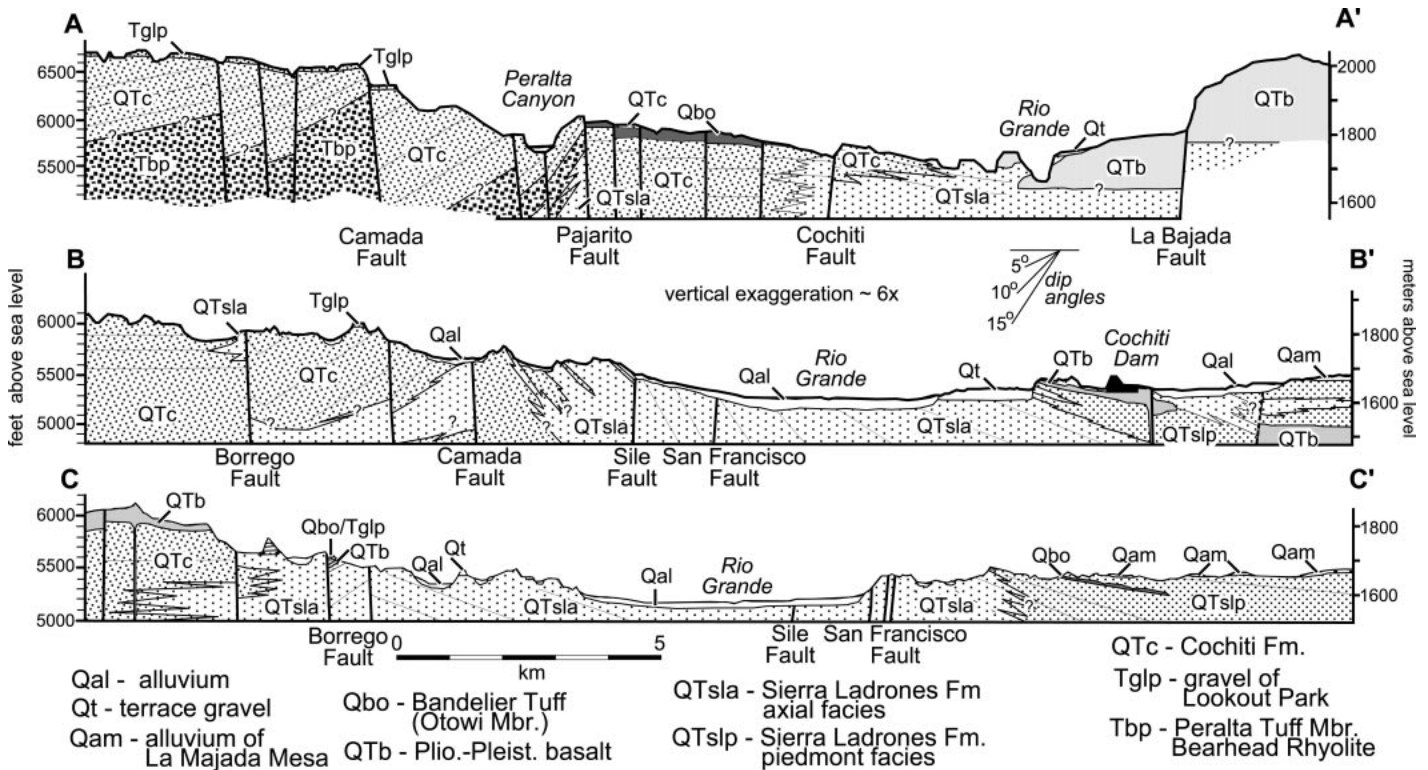


Figure 4. Geologic cross sections of the Santo Domingo basin; locations of sections are shown in Figure 3.

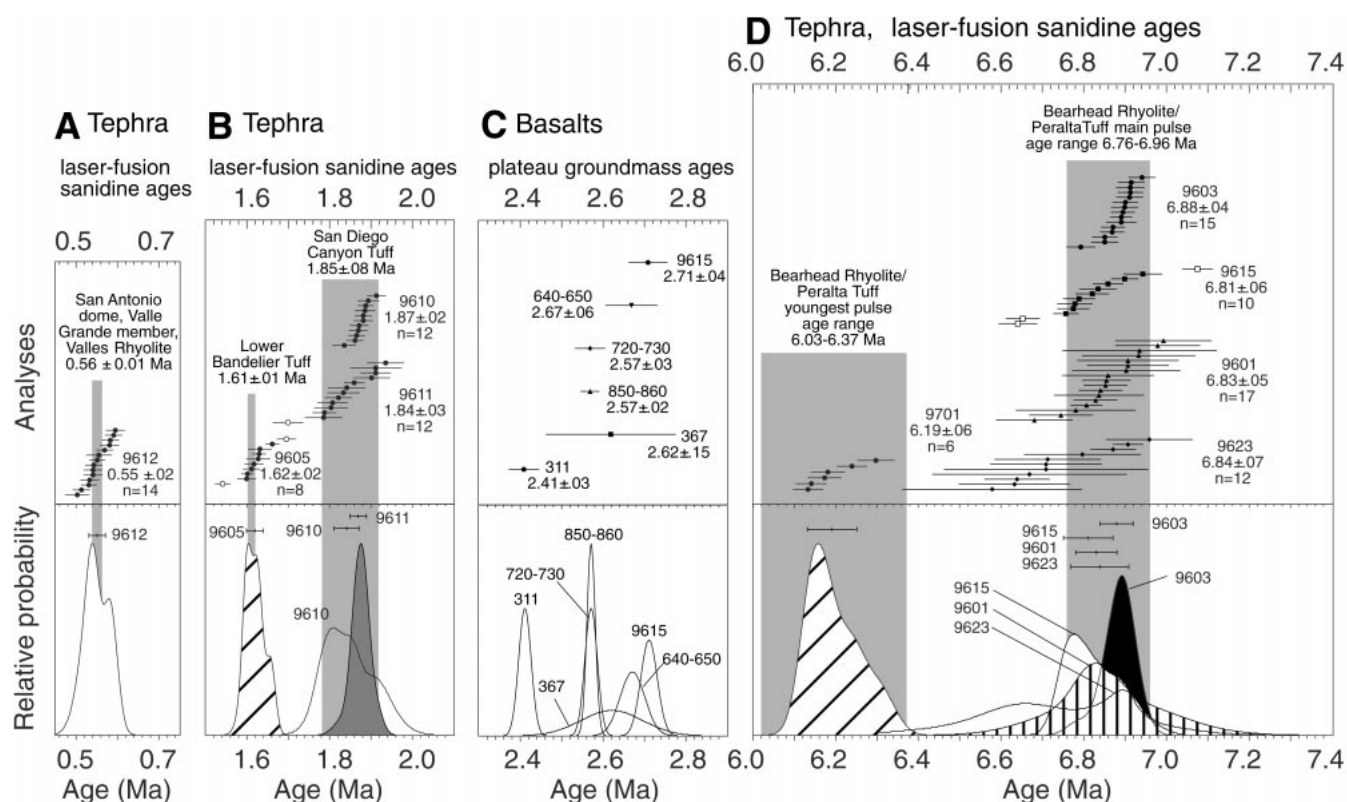


Figure 5. Probability distribution diagrams of $^{40}\text{Ar}/^{39}\text{Ar}$ results (after Deino and Potts, 1992). (A, B, D) Laser-fusion results. Lower panel shows cumulative probability, and weighted mean ages with $\pm 2\sigma$ uncertainties for each sanidine sample. Upper panel shows results for individual laser-fusion analyses. Gray bars denote ages of probable correlative eruptive units. References for ages of correlative units (all errors quoted as $\pm 2\sigma$): San Antonio dome, Valle Grande member, Valles rhyolite, 0.56 ± 0.01 Ma (Spell and Harrison, 1993); Lower Bandelier, 1.61 ± 0.01 Ma (Izett and Obradovich, 1994); San Diego Canyon Tuff, 1.85 ± 0.8 Ma (Spell et al., 1990, 1996); Bearhead Rhyolite and Peralta Tuff, youngest pulse, 6.03–6.37 Ma (McIntosh, unpublished data), oldest pulse, 6.76–6.96 Ma (McIntosh and Quade, 1995). (C) Resistance furnace incremental heating results. Lower panel shows cumulative probability, and upper panel shows plateau ages and $\pm 2\sigma$ uncertainties for each basaltic groundmass sample.

varies spatially. Devitrified rhyolite and andesite compose most clasts in the northern basin, and an abrupt upward transition from abundant glassy rhyolite to devitrified rhyolite denotes the contact with the underlying Peralta Tuff (Smith and Kuhle, 1998c). Hydrothermally altered and silicified rhyolite clasts increase upsection, from 0% at the contact with the Peralta Tuff to as much as 36%. The general upward progression from dominantly glassy rhyolite and reworked pumice in the Peralta Tuff sedimentary strata through abundant devitrified rhyolite and, penultimately, highly altered rhyolite clasts is interpreted to represent progressive dissection of Bearhead Rhyolite domes and associated pyroclastic aprons (Smith et al., 1991). Gravel in the western basin contains clasts of altered tuff and both glassy and devitrified rhyolite, derived from rhyolitic eruptive centers along the basin margin, and a variety of intermediate-composition volcanic rocks similar to those of

the Keres Group (Fig. 2). Although cobble imbrication and abrupt grain-size change indicate deposition of this gravel by eastward flows on basin-margin alluvial fans, the volcanic-clast compositions are far more diverse than the lava flows exposed along the basin margin. These clasts are, however, present within the Cerro Conejo Member of the Zia Formation west of the Cocida fault, and it seems likely that Cochiti Formation fan gravel was recycled from an older volcanoclastic apron shed southward from the Jemez Mountains synchronous with lower Keres Group volcanism and subsequently uplifted west of the Cocida fault. Further evidence for sedimentary recycling is found in the presence of nonvolcanic quartz and feldspar in some uppermost Cochiti Formation sand exposed as much as 5 km east of the Cocida fault. Similar sand is abundant in the Cerro Conejo Member in the footwall of the Cocida fault.

Consistent flow-direction indicators are un-

common in the poorly sorted Cochiti Formation, but suggest both eastward and southward dispersal, consistent with clast compositions. Interbedding of the Cochiti and Sierra Ladrones Formations in the area between Cañon Santo Domingo and Santa Ana Mesa (Fig. 3) suggest times when piedmont streams draining almost due south from the Jemez Mountains had confluences with an axial river flowing west-southwest.

The Cochiti Formation ranges from late Miocene to early Pleistocene in age, although the age of the uppermost strata varies within the basin. Near Tent Rocks, the base of the Cochiti Formation is mapped 10 m above the 6.79 Ma tuff of Cañada Camada within the Peralta Tuff (Smith et al., 1991; McIntosh and Quade, 1995), and a 6.19 Ma tephra (Table 1, sample 5) is present ~30 m above this contact. The youngest Cochiti Formation strata are in the north-central part of the basin. Tephra provisionally correlated to the San Diego

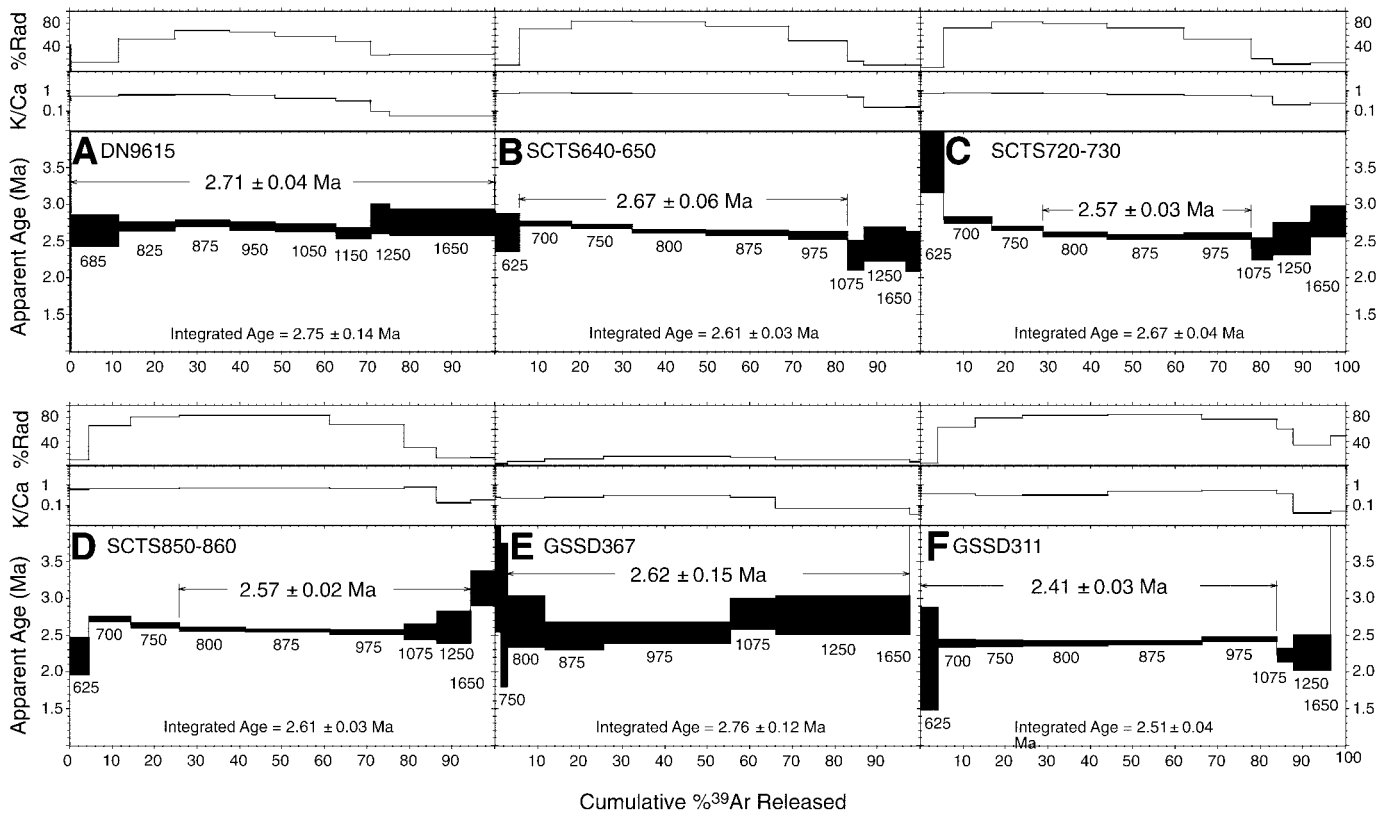


Figure 6. Age spectra for basaltic groundmass concentrate samples, including plateau ages, percent radiogenic yield of ^{40}Ar , and K/Ca, a molar ratio calculated from K-derived ^{39}Ar and Ca-derived ^{37}Ar .

Canyon ignimbrites, and dated as 1.84 and 1.87 Ma (Table 1, samples 3 and 4), are present near the top of the formation near Cochiti Lake. East of the Pajarito fault near Tent Rocks, the Otowi Member of the Bandelier Tuff (1.61 Ma) is present in the uppermost Cochiti Formation.

The Cochiti Formation is partly correlative to the Arroyo Ojito Formation, principally exposed southwest of our study area, and derived mostly from nonvolcanic source areas west and southwest of the Jemez Mountains (Connell et al., 1999). Between the Santa Ana and Cocida faults (Fig. 1), an 80-m-thick section of arkosic Arroyo Ojito Formation contains tephra correlative with the Peralta Tuff and is overlain by as much as 30 m of coarse-grained, volcanoclastic, but not tuffaceous, Cochiti Formation (Chamberlin et al., 1999). Arroyo Ojito strata may underlie and interfinger with the Cochiti Formation in the subsurface of the western part of our study area, having been deposited there by east-flowing streams that were eventually displaced southward by progradation of Cochiti Formation gravel from the Jemez Mountains and footwall uplift along the Cocida fault.

ALLUVIUM ASSOCIATED WITH PLIOCENE–PLEISTOCENE EROSION SURFACES

Santa Fe Group strata in the Santo Domingo basin are, in most places, truncated by high-level erosion surfaces, remnants of which are overlain by alluvium (Fig. 3). The alluvial strata include sand underlying dissected La Majada Mesa east of the Rio Grande, and remnants of extensive pediment gravel west of the Rio Grande. Kelley (1977) correlated both of these pediments with the Ortiz surface of Bryan (1938). The type Ortiz surface and its overlying gravel mantle are developed east of the La Bajada fault and are locally capped by 2.8 ± 0.1 Ma basalt (K-Ar date from Bachman and Mehnert, 1978, sample 7). The pediment surfaces in the Santo Domingo basin are clearly younger and should not be equated with the Ortiz surface.

Gravel of Lookout Park

Erosional remnants of high-level pediment gravel form interfluvial in the western part of the basin (Fig. 3). The underlying southeast-sloping erosion surface truncates west-dipping

Cochiti Formation and Peralta Tuff and is overlain by the 5–15-m-thick gravel of Lookout Park (named for a locality labeled on the 1978, but not 1993, edition of the Cañada 7.5' Quadrangle), which is generally coarser than the Cochiti Formation. This gravel generally occupies the highest landscape position except near Borrego Canyon, where it is inset below 2.41 Ma basalt of Santa Ana Mesa (Table 1, sample 15), and west of the Cocida fault, where it forms inverted valley fills inset below older Santa Fe Group (Chamberlin et al., 1999). In the western Santo Domingo basin, the 1.61 Ma Otowi Member of the Bandelier Tuff disconformably overlies the pediment gravel. This upper Pliocene, unconformity-bounded gravel is correlative with some part of the continuous, conformable Miocene–lower Pleistocene Santa Fe Group in the eastern Santo Domingo basin (Fig. 4).

Alluvium of La Majada Mesa

A broad geomorphic surface bisected by the Santa Fe River in the eastern Santo Domingo basin was named the La Bajada surface by Bryan (1938). To avoid confusion with the La Bajada Mesa, northeast of the La Bajada fault,

we name this surface for the La Majada Mesa, the wide interfluvium between the Santa Fe River and Galisteo Creek (Fig. 3). The gently west-sloping erosion surface truncates the east-dipping Sierra Ladrones Formation, including the lower Pleistocene Bandelier Tuff, demonstrating a younger age than the Ortiz surface. Excavations reveal that the erosion surface is overlain by bioturbated pebbly sand alluvium and local accumulations of as much as 12 m of eolian sand containing as many as 3 buried soils. The age of the alluvium of the La Majada Mesa is not clearly established, but these deposits are comparable in elevation to the highest recognized terrace along the Rio Grande, dated as ca. 660 ka (see following). The Santa Fe River and Galisteo Creek probably cut the surface during a long period of base-level stability in the middle Pleistocene.

QUATERNARY TERRACE ALLUVIUM

Four fluvial terrace levels are recognized along the Rio Grande and its principal tributaries (Table 3). A fifth (lowest) terrace is locally recognized in tributary drainages. Correlation of terraces throughout the field area was based on tread elevation above grade and relative heights between adjacent terrace treads. Although many factors may affect tread elevations, the sequence of terraces is consistent through the field area and ranges in tread elevations above grade are small (Table 3). The ages of Rio Grande terrace gravels were estimated on the basis of relationships to dated tephra layers and suggested correlations based only on elevations above grade to terraces in the Española basin, for which a calibrated amino-acid chronology has been proposed (Table 3; Dethier and McCoy, 1993). Terraces along piedmont drainages are readily projected to Rio Grande terrace treads and are similar in number and height above grade to terraces in a major tributary just north of our study area, a tributary for which Aby (1997) proposed a soil-based alluvial sequence. All terraces are of Pleistocene age and the Rio Grande currently flows on a 30-m-thick fill (Smith and Kuhle, 1998a) that comprises the modern valley floor. Apparent regional synchronicity of principal intervals of valley filling and incision suggest that the terraces formed primarily in response to cyclic Pleistocene climatic change (Dethier et al., 1988; Rogers and Smartt, 1996).

Rio Grande terraces are not widely preserved within the Santo Domingo basin (Fig. 7). Remnants of the Qt_1 terrace are restricted north of Cochiti Dam (Dethier, 1999) and in the vicinity of Santo Domingo Pueblo, where they are found in a 9-km-wide belt (compared

to 4 km for the modern flood plain). South of Cochiti Dam, the younger terraces (Qt_2 – Qt_4) are found only on the east side of the river and only north of the San Francisco fault (Fig. 7). This suggests that the river has undergone net westward migration during the past ~300 k.y. (approximate age of Qt_2 alluvium) north of the San Francisco fault and has undergone sufficient eastward and westward lateral migration farther south to remove older alluvium in the study area.

Further indication of net westward migration of the Rio Grande is observed in the relationship between the flood-plain margin and tributary-stream alluvium (Fig. 7). Erosional scallop-shaped escarpments with little or no development of tributary-mouth fans mark the western margin of the flood plain. This is most clearly seen at the mouth of Peralta Canyon, where an 8-m-high flood-plain margin scarp is cut into a previous tributary-mouth fan that was graded to a Rio Grande channel position ~1 km farther east. In contrast, broad tributary-mouth fans on the east side of the valley are graded to and encroach upon the modern flood plain.

STRUCTURAL GEOLOGY

The Santo Domingo basin within the study area has the form of a nearly symmetrical graben with an antiformal distribution of bedding attitudes (Figs. 3 and 4). Strata in the eastern part of the basin dip eastward at 5° – 10° and are associated with primarily down-to-the-west normal faults. In the western basin, strata dip westward at 10° – 15° and are deformed by down-to-the-east faults. In the north-central part of the basin, a central graben of essentially flat-lying deposits separates the domains of opposite tilt (Fig. 4A). South of the terminus of the Pajarito fault, the central graben is no longer defined and the oppositely tilted strata come into direct contact first across the Camada fault (Fig. 4B) and then farther south, close to or along the Borrego fault (Fig. 4C). A horst with nonsystematic bedding attitudes is present in the narrow zone of latitudinal overlap of the Pajarito and San Francisco faults. Most, although not all, of the faults in the basin have documented displacement of upper Pliocene or Quaternary deposits (Table 4).

Faults in the eastern basin continue southward as principal structures defining the eastern boundary of the east-tilted Albuquerque basin. The La Bajada fault has a total length of 40 km (Kelley, 1977; Machette et al., 1998) and apparently terminates ~10 km north of the area shown in Figure 3 (Smith et al., 1970; Dethier, 1999). Although Pliocene lava flows

are displaced by more than 400 m, there is no evidence of post-middle Pleistocene movement on this fault (Dethier, 1999; Machette et al., 1998), and displacement likely diminishes toward the north (D.P. Dethier, 2000, written commun.). Just east of the study area faults parallel to and east of the La Bajada structure displace older Tertiary rocks but do not offset the Pliocene lava flows of the Cerros del Rio (Sun and Baldwin, 1958; Stearns, 1953; Sawyer et al., 2000), suggesting a slightly (~2 km) wider basin during Miocene time. The San Francisco fault, of which the Sile fault is a splay, has a total length of 48 km and connects with other faults that define the deep eastern margin of the Albuquerque basin south of the terminus of the La Bajada fault (Fig. 1; Kelley, 1977; Russell and Snelson, 1994). A Quaternary displacement of more than 200 m is estimated for the San Francisco fault near Santo Domingo Pueblo (Table 3) on the basis of the presence of Bandelier Tuff pumice within Sierra Ladrones Formation gravel in the hanging wall relative to the projection of dipping Bandelier Tuff ignimbrite in the footwall. This fault system terminates to the north, somewhere south of Tent Rocks (Fig. 3).

Faults in the western basin continue northward as principal structures defining the western margin of the west-tilted Española basin half-graben. The Pajarito fault (Fig. 1) likely has the most significant late Quaternary throw and greatest net Tertiary offset (based on the thickness of basin fill inferred from gravity data), but it is not the western boundary of the rift. The western boundary is a diffuse zone of east-facing normal faults that displace the basin floor in a step-like fashion toward the deepest part of the basin east of the Pajarito fault. This western shelf of the Española basin is largely filled with volcanic rocks erupted in the Jemez Mountains and emerges to the north as the Abiquiu embayment (Fig. 1). Gardner et al. (1986) applied the name Cañada de Cochiti fault zone to this diffuse zone of western boundary faults that extends through the Jemez Mountains. The Santa Ana and Cocida faults are part of that zone and, although not continuously mapped through the Jemez Mountains, project to faults forming the western margin of the Abiquiu embayment (Fig. 1). Southward, these faults merge with a wide band of faults marking the western margin of the Albuquerque basin. The Pajarito fault clearly terminates in the northern Santo Domingo basin (Fig. 3). The Camada, Borrego, and Peralta faults appear to display decreasing displacement toward the south (Table 4); the Camada fault lacks definition west of Santo Domingo Pueblo and strands of the Borrego fault actually strike toward faults of opposite

displacement sense farther south (Kelley, 1977; Cather and Connell, 1998). The Camada and Peralta faults are important structures along the western margin of the west-tilted Bearhead basin, a feature in the southern Jemez Mountains that subsided at least 1 km during late Miocene and Pliocene time (Fig. 1; Smith, 1999). The Peralta fault is inferred to be coincident with a profound drainage lineament persisting northward to the Valles Caldera (Fig. 1).

The Santo Domingo basin is, therefore, a region of overlapping opposite-facing normal faults; the faults continue north and south as major structures at or near the margins of more strongly asymmetric basins (Fig. 1). The nature of the transfer of strain between the oppositely tilted Albuquerque and Española basins has not been clearly determined. A Santa Ana accommodation zone inferred by Cather (1992) as a complex zone of en echelon, rift-parallel faults was subsequently depicted as a discrete, northeast-striking, transverse structure by Chapin and Cather (1994), Russell and Snelson (1994), and Tedford and Barghoorn (1999). Faulds and Varga (1998) and Stewart et al. (1998) depicted a series of en echelon, rift-parallel antithetic, antiformal accommodation zones across a broad area of the northern Albuquerque and Santo Domingo basins. Dip reversals along antiformal welts are present elsewhere in the northern Albuquerque basin, but it is the Santo Domingo basin that is clearly defined by the overlap of faults active since late Miocene time; the faults continue longitudinally to form the margins of the adjacent asymmetric basins (Fig. 1). We suggest, therefore, that the Santo Domingo basin, while possibly not accounting for all of the transfer of strain between the Albuquerque and Española basins, is the principal expression of the accommodation zone between them. Although it is largely an antithetic anticlinal strike-parallel accommodation zone in the classification of Faulds and Varga (1998), the geometry of the axial welt varies longitudinally within the basin. In the northern basin, the axial welt has collapsed to form a key-stone-like graben between the Pajarito and Cochiti faults (Fig. 4A). As these faults lose definition to the south, a horst is formed in the area of overlap of the Pajarito and San Francisco–Sile faults, followed farther south by a low-amplitude anticline, the axis of which is along and southwest of the Camada fault (Fig. 4, B and C).

INFERRED SUBSIDENCE HISTORY

Analyses of paleocourses of the axial river, along with the development of erosional sur-

TABLE 3. DESCRIPTION AND AGE OF RIO GRANDE TERRACE DEPOSITS

Terrace	Height of tread above modern channel (m)	Description	Age
Qt ₁	75–85	Gravel, 3–5 m thick locally capped by a discontinuous veneer of eolian sand and silt to 0.5 m. Correlative terraces found along several western piedmont drainages.	Contains, near the base, a reworked pale-gray ash correlated on the basis of shard chemistry (A. Sarna-Wojcicki, U.S. Geological Survey, March 1998, written commun.) to Lava Creek B (660 ka; Izett et al., 1992; Lanphere et al., 1999).
Qt ₂	65–70	Gravel and silty sand with buried soils; 1.5–5 m thick. Correlative piedmont terraces sparsely preserved along Santa Fe River and near mouth of Borrego Canyon. Along Cochiti Lake includes volcanic boulders to 3 m across that presumably represent floods related to outbreaks from landslide dams in White Rock Canyon, north of area depicted in Figure 3.	Lower part of fill contains reworked 550 ka Valles Rhyolite tephra (Table 1, sample 1). Amino acid ratios for gastropods suggest an age of 250–300 ka (Dethier, 1999). Dethier and McCoy (1993) estimate an age of 310 ± 70 ka for terrace deposits at 70–90 m above grade near Española.
Qt ₃	35–40	Forms a 30-m-thick fill between Cochiti Dam and Peña Blanca. The fill consists of three intervals, from bottom to top: (1) cobble gravel with intercalated sand lenses and minor slack-water silt and clay (15 m); (2) sand and silt with gravel lenses and local gypsiferous mud (12–15 m); (3) gravel (1–2 m). Correlative piedmont terrace fills generally <10 m thick and most prominent along Peralta Canyon, Santa Fe River, Galisteo Creek, Borrego Canyon, and marking a former course of Peralta Canyon through the central basin.	Dethier and McCoy (1993) estimated an age of 170 ± 40 ka for fill terraces at 40–50 m above grade in the Española basin.
Qt ₄	15–18	Gravel, 15–25 m thick between Cochiti Dam and Peña Blanca. Capped by eolian and sheathwash sand and silt. Near Cochiti Dam includes boulders of basalt to 4 m across that presumably represent floods related to outbreaks from landslide dams in White Rock Canyon, north of area depicted in Figure 3. Correlative piedmont terrace fills generally <10 m thick and most prominent along Peralta Canyon, Santa Fe River, Galisteo Creek, Cañon Santo Domingo, and Borrego Canyon	Overlain by ca. 60 ka El Cajete Pumice (Reneau et al., 1996). Dethier and McCoy (1993) estimated an age of 95 ± 15 ka for fill terraces at 15–20 m above grade in the Española basin.

faces and patterns of terrace preservation, are used to interpret patterns of subsidence and faulting in the Santo Domingo basin. We assume that the shifting facies tract of the axial river, by marking the topographically lowest part of the basin floor, permits identification of time intervals in which dominantly eastward or westward tilting of the basin floor was

occurring following the work of Bridge and Mackay (1993) and Leeder et al. (1996). In addition, we assume that the formation across fault traces of low-relief erosion surfaces capped by even thickness of alluvium will not occur if there is significant movement on those faults. Such displacement would produce a topographically irregular surface with

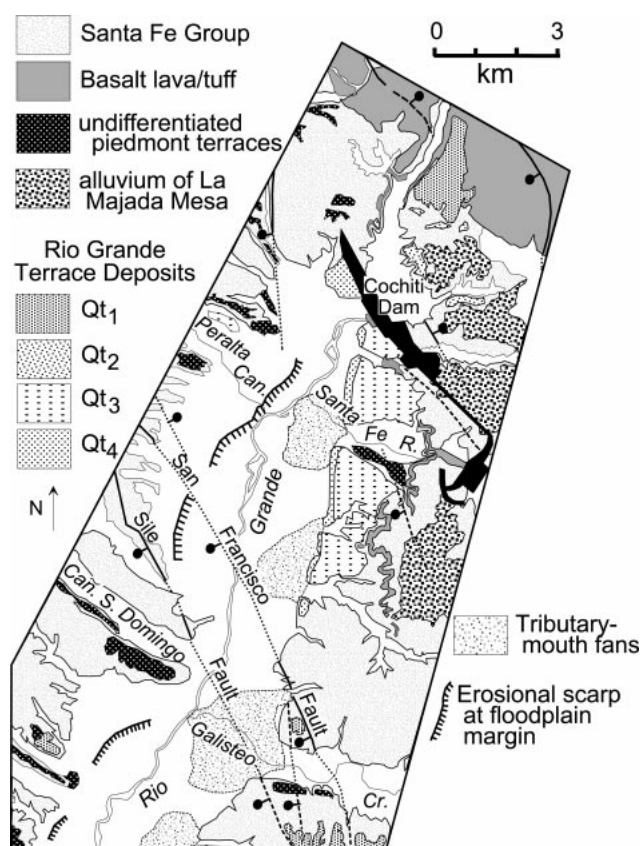


Figure 7. Terraces and modern fluvial-geomorphic features along the Rio Grande valley. See Table 3 for descriptions of terrace deposits.

local accumulation of scarp-derived colluvium and accommodation of thicker alluvium on hanging-wall blocks.

Pre-late Miocene subsidence patterns cannot be readily gleaned from the data currently available. Older strata are exposed only west of the Cocida fault and east of the La Bajada fault. The almost complete restriction of younger sedimentary strata in the hanging walls of these faults suggests a wider basin at an earlier time, but details of its subsidence history are unknown.

Late Miocene to Early(?) Pliocene

Stratigraphic and facies relationships suggest that the current western margin of the Santo Domingo basin formed in the late Miocene during a period of strong westward tilting of the basin floor (Fig. 8A). West of the Cocida fault, a section of the Arroyo Ojito Formation containing primary and reworked Peralta Tuff pyroclastic debris is only 50 m thick (Chamberlin et al., 1999), in contrast with more than 500 m of sedimentary section coeval with the Peralta Tuff in the west-central Santo Domingo basin. More than 600 m of Cochiti Formation west of Tent Rocks is cor-

relative to only 30 m of Cochiti Formation found locally in the hanging wall of the Santa Ana fault. Although these latter outcrops may record formation of alluvial fans along the Santa Ana fault, maximum subsidence and accommodation of sedimentary section were clearly focused east of the active Cocida fault.

The course of the axial river was displaced westward in the basin in late Miocene time. In the Española basin, the westward margin of the flood plain must have remained east of volcanic highlands in the eastern Jemez Mountains (Fig. 1). The presence of pre-7 Ma axial gravel in the subsurface northwest of Tent Rocks (Gay and Smith, 1996) requires, therefore, a minimum of 15 km of westward shift in the course of the river over a north to south distance of no more than 5 km. Outcrops in Peralta Canyon show that the river was 7.5 km west of its present position ca. 6.8 Ma. The location of the axial river within the western part of the basin suggests westward tilting of the basin floor. It is notable that the Camada and Peralta faults in the western basin form the stepped boundary to the west-tilted Bearhead basin block within the Jemez Mountains, which was clearly subsiding contemporaneously with eruption of the Peralta

Tuff Member of the Bearhead Rhyolite (Smith, 1999).

Late Pliocene to Early Pleistocene

The deposition of the youngest basin-fill sediment in the eastern basin and contemporaneous formation of an erosion surface in the western basin indicate a Pliocene transition from westward tilting to eastward tilting (Fig. 8B). The development of the erosion surface capped by the gravel of Lookout Park post-dates eruption of basalts capping Santa Ana Mesa and dated as 2.67–2.41 Ma (Table 1, samples 14–15). The 2.41 Ma basalt overlies the Cochiti Formation, which is notable for buried soils in its uppermost part, possibly signaling an overall decrease in sedimentation rates in the western basin at that time. The erosion surface and overlying gravel project eastward into a conformable Sierra Ladrone Formation section that includes at least 150 m of post-2.6 Ma section (Fig. 4) and, in the Galisteo Creek area, at least 35 m of post-1.61 Ma section. Axial gravel is found in wells as much as 8.5 km east of the present river (Fig. 4B). Therefore, eastward tilting of the basin floor caused the ancestral Rio Grande to shift toward the eastern basin and also caused erosional beveling of strata in the western basin. Streams that transported sediment eastward to the subsiding and aggrading eastern basin formed the resulting erosion surface beneath the gravel of Lookout Park. Pedimentation in the western basin demonstrates base-level stability and axial-stream aggradation equal and opposite to the rate of basin subsidence. These conditions persisted into early Pleistocene time, as indicated by (1) the presence of the Otowi Member of the Bandelier Tuff within the Sierra Ladrone Formation in the eastern basin, and (2) its restriction to erosional remnants perched disconformably above the gravel of Lookout Park in the western basin (Figs. 4 and 8B).

Eastward tilting was probably accomplished primarily by motion along the La Bajada and San Francisco faults. Lava flows thought to correlate to those in the footwall of the La Bajada fault are found at a depth of 150 m below the La Majada Mesa surface (Table 1, samples 11–13), suggesting at least 425 m of post-2.6 Ma throw (Fig. 4; Table 3). In the absence of evidence for post-middle Pleistocene activity on the La Bajada fault (Machette et al., 1998), the observed displacement must have occurred in Pliocene and early Pleistocene time. Early Pleistocene motion on the San Francisco fault is indicated by at least 200 m of post-1.61 Ma throw and lack of displacement of the ca. 660 ka Qt_1 terrace. Both

TABLE 4. FAULT DISPLACEMENTS IN THE SANTO DOMINGO BASIN

Location*	Dip separation (m)	Displaced stratigraphic unit	Age of displaced stratigraphic unit
Borrogo fault zone			
1	40	Gravel of Lookout Park	Late Pliocene
2	25	Gravel of Lookout Park	Late Pliocene
3	30	Basalt of Santa Ana Mesa	2.41 Ma
4	25	Basalt of Santa Ana Mesa	2.41 Ma
Camada fault			
5	280	Peralta Tuff Member of Bearhead Rhyolite	6.79 Ma tuff of Cañada Camada
	66	Gravel of Lookout Park	Late Pliocene
	>10	Tshierge Member of Bandelier Tuff	1.22 Ma
6	62	Gravel of Lookout Park	Late Pliocene
7	>650	Peralta Tuff Member of Bearhead Rhyolite	6.7–6.9 Ma
8	20	Gravel of Lookout Park	Late Pliocene
9	<10	Gravel of Lookout Park	Late Pliocene
Pajarito fault			
10	>90	Otowi Member of Bandelier Tuff	1.61 Ma
11	14	Qt ₄ fill terrace	ca. 95 ka
San Francisco / Sile fault			
12	>80	Sierra Ladrones Fm. Gravel containing Peralta Tuff pumice	ca. 6.8 Ma
13	>200	Otowi Member, Bandelier Tuff and axial gravel with Bandelier pumice	1.61 Ma
	~0	Qt ₁ terrace gravel	ca. 660 ka
Cochiti fault			
14	>80	Cochiti Formation With pumice correlative with San Diego Canyon ignimbrite	ca. 1.85 Ma
	~50	Otowi Member, Bandelier Tuff	1.61 Ma
	~0	Qt ₄ fill terrace	ca. 95 ka
Faults near Cochiti Dam & Peña Blanca			
15	70	Sierra Ladrones Fm. Containing basalt flow	2.71 Ma
	0	Alluvium of La Majada Mesa	ca. 0.6–1.0 Ma
16	25	Sierra Ladrones Formation Containing basalt flow	2.71 Ma
	0	Alluvium of La Majada Mesa	ca. 0.6–1.0 Ma
La Bajada fault			
17	~425	Pliocene basalt	ca. 2.5–2.6 Ma
	~0	Middle Pleistocene terrace and landslide deposits along strike	ca. 0.3 Ma

*Figure 3.

west-dipping and east-dipping faults in the Peña Blanca–Cochiti Dam area also displace 2.7 Ma basalt flows, but do not disrupt the La Majada Mesa surface or Pleistocene terrace gravel (Smith and Kuhle, 1998a; Table 3). Aeromagnetic data suggest the presence of one or more concealed faults beneath the La Majada Mesa surface, north of the Santa Fe River (U.S. Geological Survey et al., 1999).

The time interval required for the axial river to relocate its course from the western to eastern basin is not known, because the base of the axial gravel in the eastern basin is not exposed. North of Santa Ana Mesa, axial-river gravel facies are found as much as 15 km west of the Rio Grande at a stratigraphic level ~30 m below the 2.41 Ma basalt forming the north edge of the mesa. These presumably Pliocene gravel layers are not common north of Cañon Santo Domingo (Fig. 3); in the vicinity of the canyon, relations with the Cochiti Formation suggest confluences between southward-flowing piedmont streams and a west-southwest-flowing ancestral Rio Grande. Exclusion of the axial river from the northwestern basin, where it was present prior to 7 Ma, may result both from progradation of piedmont gravel along fault-parallel drainage courses and uplift of the intrabasinal high between the Sile and Pajarito faults (Figs. 3 and 4).

The central keystone graben in the northern basin was apparently well developed, and may have formed at this time. The Otowi Member of the Bandelier Tuff is near the top, but within, the Cochiti Formation east of the Pajarito fault, but unconformably overlies the gravel of Lookout Park in the footwall. The Cochiti fault, on the east side of the keystone graben, exhibits about 50 m of displacement of Bandelier Tuff. Tephra correlated to the San Diego Canyon ignimbrites (ca. 1.85 Ma) is well preserved within Cochiti Formation in the footwall of the Cochiti fault (Table 1, samples 3–4), but has not been found in the dissected fill to the west, suggesting >70 m of throw on this upper Pliocene marker and implying Pliocene motion on the fault.

Middle Pleistocene to Present

Several observations suggest that the basin is currently undergoing a transition back to dominantly westward tilt (Fig. 8C). The evidence for this interpretation is mostly geomorphic, because the Santa Fe Group deposition ceased in early Pleistocene time and was followed by base-level fall and incision of the Rio Grande. The formation of very broad erosion surfaces, represented by the basal strath of the ca. 660 ka Qt₁ terrace gravel and that below the La Majada Mesa surface (Fig. 7),

suggests an extended period of local base-level stability, possibly representing a balance between subsidence in the eastern basin and regional base-level fall. If so, this was probably at about the end of significant motion on faults in the eastern basin, for which there is no evidence of post-middle Pleistocene movement. In the western basin, the gravel of Lookout Park is offset by all but one mapped east-dipping fault, indicating post-early Pleistocene faulting of that region of the basin that was relatively stable during late Pliocene pedimentation. Offset of an upper Pleistocene Qt₄ tributary-terrace gravel by the Pajarito fault (Table 4) indicates that at least one of these structures moved after cessation of motion on faults in the eastern basin. Downstream convergence of Qt₃ and Qt₄ terraces in Borrogo Canyon (Smith and Kuhle, 1998b) is consistent with post-300 ka motion along splays of the Borrogo fault.

Terrace preservation along the Rio Grande in the north-central basin indicates net westward migration of the Rio Grande, also consistent with westward tilting of the basin floor. At the north end of the basin, the river is incised into basalt flows that control the position

of the channel (Dethier, 1999). At Cochiti Dam, however, the river flows due west through an area lacking basalt flows at the surface and reestablishes a southerly course in a more westerly position. The restricted preservation of fill terraces on the east side of the valley and the discontinuous erosional escarpment along the west side of the valley indicate net westward migration of the channel over the past 300 k.y. (Fig. 7). The terraces along the Rio Grande lack piedmont-stream deposits and there are no significant piedmont streams on the east side of the valley near Cochiti Dam, where the river course shifts westward. Therefore, it is unlikely that alluvial contributions from eastern-piedmont streams deflected the river westward, leaving basin-floor tilting as the most tenable explanation for migration of the channel.

CONCLUSIONS

The Santo Domingo basin is an accommodation-zone basin, formed by the overlap of faults that continue along strike to form the boundaries of oppositely tilted, asymmetric graben. The overlapping faults not only form

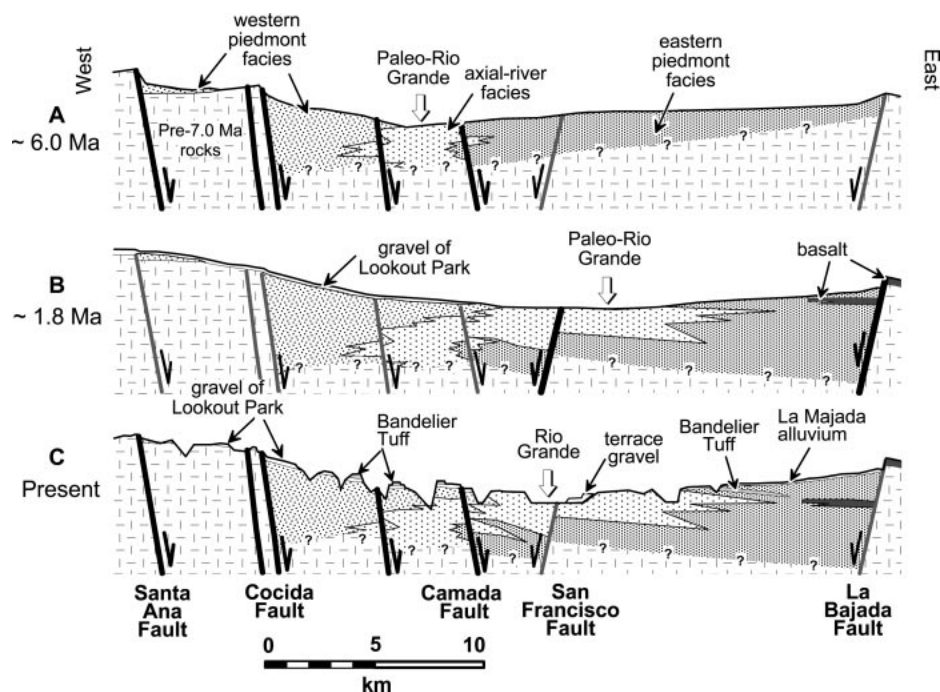


Figure 8. Schematic illustration of three-phase tilting history of the Santo Domingo basin. No vertical scale is implied because thicknesses are approximate and thicknesses of thin deposits have been exaggerated. The diagrams generalize relationships in the vicinity of cross-sections B–B' and C–C' of Figure 4. Nature of pre-7.0 Ma strata between the Cocida and La Bajada faults is unknown. (A) Late Miocene tilting was dominantly westward to account for position of axial-gravel facies of the ancestral Rio Grande in the western basin and accumulation of thick western-piedmont facies (principally Cochiti Formation and Peralta Tuff) east of the Cocida fault zone. (B) Tilting during Pliocene and early Pleistocene time was primarily to the east, accounting for the youngest basin-fill sediment having accumulated east of the modern Rio Grande. An erosion surface, capped by gravel of Lookout Park, formed in the western basin, and beveled the thick section that accumulated during late Miocene time. The unconformity-bounded gravel of Lookout Park and Bandelier Tuff (Otowi Member) in the western basin are correlative with the continuous basin-fill succession, which includes Bandelier Tuff, in the eastern basin. (C) Renewed westward tilting since the middle Pleistocene is inferred by faulting of the gravel of Lookout Park, westward migration of the Rio Grande (indicated in part by unpaired terraces on the east side of the valley), and apparent antiquity of fault movement in the eastern basin.

the basin margins, but also are interleaved within the basin with east-dipping faults diminishing in throw toward the south and west-dipping faults diminishing in importance to the north (Fig. 3; Table 3).

This study suggests that the seesaw subsidence history of accommodation zones formed by overlapping half-graben proposed by Rosendahl (1987) is consistent with facies patterns and data constraining timing of fault movement. The postulated three-phase subsidence history not only accounts for the deposition of basin-filling sediment, but also the formation of erosion surfaces and preservation of fluvial terrace deposits. Similar application of sedimentological and geomorphic analyses may reveal subsidence histories in other ba-

sins that, like the Santo Domingo basin, lack subsurface data that would permit less ambiguous interpretation. Such investigations may not only be useful for neotectonic analyses in tectonically active regions, but may elucidate patterns of deposition of aquifer and reservoir facies within accommodation zones. In the Santo Domingo basin, seesaw subsidence has distributed the most important regional aquifer material, the axial-gravel facies, more widely across the basin than if it had subsided as a half-graben (Smith and Kuhle, 1998c).

ACKNOWLEDGMENTS

Mapping upon which this paper is based was undertaken with support from the New Mexico Bureau

of Mines and Mineral Resources (NMBMMR) and the U.S. Geological Survey (USGS) under the auspices of the STATEMAP program and the Middle Rio Grande Basin Mapping Project. We especially thank Paul Bauer (NMBMMR) and David Sawyer (USGS) for logistical support and technical commentary on our work. The governors and tribal councils of Cochiti and Santo Domingo Pueblos graciously provided access to pueblo lands comprising nearly all of the study area. We appreciate the extremely helpful reviews provided by David Dethier, Frank Pazzaglia, Steven Cather, Sean Connell, and Scott Minor.

REFERENCES CITED

- Aby, S.B., 1997, The terraces of Cochiti Canyon: Soil development and relation to activity in the Pajarito fault zone [M.S. thesis]: Albuquerque, University of New Mexico, 159 p.
- Alexander J., Bridge, J.S., Leeder, M.R., Collier, R.E.L., and Gawthorpe, R.L., 1994, Holocene meander belt evolution in an active extensional basin, southwestern Montana, U.S.A.: *Journal of Sedimentary Research*, v. B64, p. 542–559.
- Bachman, G.O., and Mehnert, H.H., 1978, New K-Ar dates and the late Pliocene to Holocene geomorphic history of the Rio Grande region, New Mexico: *Geological Society of America Bulletin*, v. 89, no. 2, p. 282–292.
- Blair, T.C., and McPherson, J.G., 1994, Historical adjustments by Walker River to lake-level fall over a tectonically tilted half-graben floor, Walker Lake basin, Nevada: *Sedimentary Geology*, v. 92, p. 7–16.
- Bridge, J.S., and Leeder, M.R., 1981, A simulation model of alluvial stratigraphy: *Sedimentology*, v. 26, p. 617–644.
- Bridge, J.S., and Mackey, 1993, A revised alluvial stratigraphy model, in Marzo, M., and Puigdefábregas, C., eds., *Alluvial sedimentation: International Association of Sedimentologists Special Publication 17*, p. 319–336.
- Bryan, K., 1938, Geology and ground water conditions of the Rio Grande depression in Colorado and New Mexico: *Rio Grande Joint Investigations in Upper Rio Grande Basins*, v. 1, pt. 2, sec. 1, p. 196–225.
- Cather, S.M., 1992, Suggested revisions to the Tertiary tectonic history of north-central New Mexico, in Lucas, S.G., et al., eds., *San Juan basin IV: New Mexico Geological Society, 43rd Field Conference, Guidebook*, p. 109–122.
- Cather, S.M., and Connell, S.D., 1998, Geologic map of the San Felipe Pueblo Quadrangle, Sandoval County, New Mexico: New Mexico Bureau of Mines and Mineral Resources Digital Open-File Map OFDM 19, 1 sheet, scale 1:24 000.
- Chamberlin, R., Pazzaglia, F.J., Wegmann, K., and Smith, G.A., 1999, Geologic map of the Loma Creston Quadrangle, Sandoval County, New Mexico: New Mexico Bureau of Mines and Mineral Resources Digital Open-File Map OFDM 25, 1 sheet, scale 1:24 000.
- Chapin, C.E., and Cather, S.M., 1994, Tectonic setting of axial basins of the northern and central Rio Grande rift, in Keller, G.R., and Cather, S.M., eds., *Basins of the Rio Grande rift: Structure, stratigraphy, and tectonic setting: Geological Society of America Special Paper 291*, p. 5–25.
- Connell, S.D., Koning, D.J., and Cather, S.M., 1999, Revisions to the stratigraphic nomenclature of the Santa Fe Group, northwestern Albuquerque basin, New Mexico, in Pazzaglia, F.J., et al., eds., *Albuquerque Country III: New Mexico Geological Society, 50th Fall Field Conference, Guidebook*, p. 337–353.
- Deino, A., and Potts, R., 1990, Single-crystal $^{40}\text{Ar}/^{39}\text{Ar}$ dating of the Ologesaillie Formation, Southern Kenya Rift: *Journal of Geophysical Research*, v. 95, p. 8453–8470.
- Deino, A., and Potts, R., 1992, Age-probability spectra from examination of single-crystal $^{40}\text{Ar}/^{39}\text{Ar}$ dating re-

- sults: Examples from Ologresalie, Southern Kenya Rift: *Quaternary International*, v. 13/14, p. 47–53.
- Dethier, D.P., 1999, Quaternary evolution of the Rio Grande near Cochiti Lake, northern Santo Domingo basin, New Mexico, *in* Pazzaglia, F.J., et al., eds., *Albuquerque geology: New Mexico Geological Society, 50th Field Conference, Guidebook*, p. 371–378.
- Dethier, D.P., and McCoy, W.D., 1993, Aminostratigraphic relations and age of Quaternary deposits, northern Española basin, northern New Mexico: *Quaternary Research*, v. 39, p. 222–230.
- Dethier, D.P., Harrington, C.D., and Aldrich, M.J., 1988, Late Cenozoic rates of erosion in the western Española basin, New Mexico: Evidence from geologic dating of erosion surfaces: *Geological Society of America Bulletin*, v. 100, no. 6, p. 928–937.
- Faulds, J.E., and Varga, R.J., 1998, The role of accommodation zones and transfer zones in the regional segmentation of extended terranes, *in* Faulds, J.E., and Stewart, J.H., eds., *Accommodation zones and transfer zones: The regional segmentation of the Basin and Range province: Geological Society of America Special Paper 323*, p. 1–46.
- Gardner, J.N., Goff, F., Garcia, S., and Hagan, R.C., 1986, Stratigraphic relations and lithologic variations in the Jemez volcanic field, New Mexico: *Journal of Geophysical Research*, v. 91, p. 1763–1778.
- Gay, K.R., and Smith, G.A., 1996, Simultaneous phreatomagmatic and magmatic rhyolitic eruptions recorded in the late Miocene Peralta Tuff, Jemez Mountains, New Mexico, *in* Goff, F., et al., eds., *The Jemez Mountains region: New Mexico Geological Society, 47th Field Conference, Guidebook*, p. 243–250.
- Grauch, V.J.S., Gillespie, C.L., and Keller, G.R., 1999, Discussion of new gravity maps for the Albuquerque basin area, *in* Pazzaglia, F.J., et al., eds., *Albuquerque geology: New Mexico Geological Society, 50th Field Conference, Guidebook*, p. 119–124.
- Heywood, C.E., 1992, Isostatic residual gravity anomalies of New Mexico: U.S. Geological Survey Water Resources Investigation Report 91–4065, 27 p.
- Izett, G.A., and Obradovich, J.D., 1994, $^{40}\text{Ar}/^{39}\text{Ar}$ age constraints for the Jaramillo normal subchron and the Matayama-Brunhes geomagnetic boundary: *Journal of Geophysical Research*, v. 99, p. 2925–2934.
- Izett, G.A., Pierce, K.L., Naeser, N.D., and Jaworowski, C., 1992, Isotopic dating of Lava Creek B tephra in terrace deposits along the Wind River, Wyoming: Implications for the post 0.6 Ma uplift of the Yellowstone hotspot: U.S. Geological Survey Open-File Report 92–391, 33 p.
- Kelley, V.C., 1977, *Geology of the Albuquerque basin, New Mexico: New Mexico Bureau of Mines and Mineral Resources Memoir 33*, 59 p.
- Lanphere, M.A., Champion, D.E., Clyne, M.A., and Muffler, L.J.P., 1999, Revised age of the Rockland tephra, northern California: Implications for climate and stratigraphic reconstructions in the western United States: *Geology*, v. 27, p. 135–138.
- Leeder, M.R., and Gawthorpe, R.L., 1987, Sedimentary models for extensional tilt block/half-graben basins, *in* Coward, M.P., et al., eds., *Continental extensional tectonics: Geological Society [London] Special Publication 28*, p. 139–152.
- Leeder, M.R., and Mack, G.H., Peakall, J., and Salyards, S.L., 1996, First quantitative test of alluvial stratigraphic models: Southern Rio Grande rift, New Mexico: *Geology*, v. 24, p. 87–90.
- Lozinsky, R.P., 1994, Cenozoic stratigraphy, sandstone petrology, and depositional history of the Albuquerque Basin, central New Mexico, *in* Keller, G.R., and Cather, S.M., eds., *Basins of the Rio Grande rift: Structure, stratigraphy, and tectonic setting: Geological Society of America Special Paper 291*, p. 73–82.
- Machette, M.N., Personius, S.F., Kelson, K.L., Haller, K.M., and Dart, R.L., 1998, Map and data for Quaternary faults and folds in New Mexico: U.S. Geological Survey Open-File Report 98–521, 443 p., scale 1:750 000.
- Mack, G.H., and Seager, W.R., 1990, Tectonic control on facies distribution of the Camp Rice and Palmas Formations (Pliocene-Pleistocene) in the southern Rio Grande rift: *Geological Society of America Bulletin*, v. 102, p. 45–53.
- McIntosh, W.C., and Chamberlin, R.M., 1994, $^{40}\text{Ar}/^{39}\text{Ar}$ geochronology of middle to late Cenozoic ignimbrites, mafic lavas and volcanoclastic rocks in the Quemado-Datil region, New Mexico, *in* Chamberlin, R.M., Kues, B.S., Cather, S.M., Barker, J.M., McIntosh, W.C., eds., *Mogollon slope, west-central New Mexico and east-central Arizona: New Mexico Geological Society Guidebook, 45th Field Conference*, p. 165–186.
- McIntosh, W.C., and Quade, J., 1995, $^{40}\text{Ar}/^{39}\text{Ar}$ geochronology of tephra layers in the Santa Fe Group, Española basin, New Mexico, *in* Bauer, P.W., et al., eds., *Geology of the Santa Fe region: New Mexico Geological Society, 46th Field Conference, Guidebook*, p. 279–287.
- Morley, C.K., Nelson, R.A., Patton, T.L., and Munn, S.G., 1990, Transfer zones in the East African rift system and their relevance to hydrocarbon exploration in rifts: *American Association of Petroleum Geologists Bulletin*, v. 74, p. 1234–1253.
- Peakall, J., 1998, Axial river evolution in response to half-graben faulting: Carson River, Nevada, U.S.A.: *Journal of Sedimentary Research*, v. 68, p. 788–799.
- Purtymun, W.D., 1995, Geologic and hydrologic records of observation wells, test holes, test wells, supply wells, springs, and surface water in the Los Alamos area: Los Alamos National Laboratory Report LA-12883-MS, 339 p.
- Reneau, S.L., Gardner, J.N., and Forman, S.L., 1996, New evidence for the age of the youngest eruptions in the Valles caldera, New Mexico: *Geology*, v. 24, p. 7–10.
- Rogers, J.B., and Smartt, R.A., 1996, Climatic influences on Quaternary alluvial stratigraphy and terrace formation in the Jemez River valley, New Mexico, *in* Goff, F., Kues, B.S., Rogers, M.A., McFadden, L.D., and Gardner, J.N., eds., *The Jemez Mountains region: New Mexico Geological Society Guidebook 45th Field Conference*, p. 347–356.
- Rosendahl, B.R., 1987, Architecture of continental rifts with special reference to East Africa: *Annual Review of Earth and Planetary Sciences*, v. 15, p. 445–503.
- Russell, L.R., and Snelson, S., 1994, Structure and tectonics of the Albuquerque basin segment of the Rio Grande rift: Insights from seismic reflection data, *in* Keller, G.R., and Cather, S.M., eds., *Basins of the Rio Grande rift: Structure, stratigraphy, and tectonic setting: Geological Society of America Special Paper 291*, p. 83–112.
- Samson, S.D., and Alexander, C.E., 1987, Calibration of the interlaboratory $^{40}\text{Ar}/^{39}\text{Ar}$ dating standard, Mmhb-1: *Isotope Geoscience*, v. 66, p. 27–34.
- Sawyer, D.A., Shroba, R.R., Minor, S.A., Thompson, R.A., and Blossom, J.C., 2000, Geologic map of the Tetilla Peak Quadrangle, Santa Fe and Sandoval Counties, New Mexico: U.S. Geological Survey Miscellaneous Field Studies Map MF-2352, scale 1:24 000.
- Smith, G.A., 1999, Tectonics and volcanism of the late Miocene Bearhead magmatic episode in the southeastern Jemez Mountains, New Mexico [abs.]: *New Mexico Geology*, v. 21, p. 37–38.
- Smith, G.A., and Kuhle, A.J., 1998a, Geologic map of the Santo Domingo Pueblo Quadrangle, Sandoval County, New Mexico: New Mexico Bureau of Mines and Mineral Resources Open-File Digital Map OFDM 15, 1 sheet, scale 1:24 000.
- Smith, G.A., and Kuhle, A.J., 1998b, Geologic map of the Santo Domingo Southwest Quadrangle, Sandoval County, New Mexico: New Mexico Bureau of Mines and Mineral Resources Open-File Digital Map OFDM 26, 1 sheet, scale 1:24 000.
- Smith, G.A., and Kuhle, A.J., 1998c, Hydrostratigraphic implications of new geological mapping in the Santo Domingo Basin: *New Mexico Geology*, v. 20, p. 21–27.
- Smith, G.A., and Lavine, A., 1996, What is the Cochiti Formation?: *New Mexico Geological Society, 47th Field Conference, Guidebook*, p. 219–224.
- Smith, G.A., Larsen, D., Harlan, S.S., McIntosh, W.C., Erskine, D.W., and Taylor, S., 1991, A tale of two volcanoclastic aprons: Field guide to the sedimentology and physical volcanology of the Oligocene Espinosa Formation and Miocene Peralta Tuff, north-central New Mexico: *New Mexico Bureau of Mines and Mineral Resources, Socorro, Bulletin 137*, p. 87–103.
- Smith, G.A., Simmons, M.C., and Kuhle, A.J., 1997, Contemporaneous magmatic and hydromagmatic Pliocene basalt eruptions at the site of Cochiti Dam, Sandoval County, New Mexico [abs.]: *New Mexico Geology*, v. 19, p. 63.
- Smith, R.L., Bailey, R.A., and Ross, C.S., 1970, Geologic map of the Jemez Mountains, New Mexico: U.S. Geological Survey Miscellaneous Investigations Map I-571, scale 1:125 000.
- Spell, T.L., and Harrison, T.M., 1993, $^{40}\text{Ar}/^{39}\text{Ar}$ geochronology of post-Valles Caldera rhyolites, Jemez volcanic field, New Mexico: *Journal of Geophysical Research*, v. 98, p. 8031–8051.
- Spell, T.L., Harrison, T.M., and Wolff, J.A., 1990, $^{40}\text{Ar}/^{39}\text{Ar}$ dating of the Bandelier Tuff and San Diego Canyon ignimbrites, Jemez Mountains, New Mexico; temporal constraints on magmatic evolution: *Journal of Volcanology and Geothermal Research*, v. 43, p. 175–193.
- Spell, T.L., McDougall, I., and Dougeris, A., 1996, The Cerro Toledo Rhyolite, Jemez Volcanic Field, New Mexico: $^{40}\text{Ar}/^{39}\text{Ar}$ chronology of the transition between two caldera-forming eruptions: *Geological Society of America Bulletin*, v. 108, p. 1549–1566.
- Stearns, C.E., 1953, Early Tertiary volcanism in the Galisteo-Tongue area, New Mexico: *American Journal of Science*, v. 251, p. 415–452.
- Steiger, R.H., and Jäger, E., 1977, Subcommission on geochronology: Convention on the use of decay constants in geo- and cosmochronology: *Earth and Planetary Science Letters*, v. 36, p. 359–362.
- Stewart, J.H., Anderson, R.E., Arranda-Gómez, J.J., Beard, L.S., Billingsley, G.H., Cather, S.M., Dilles, J.H., Dokka, R.K., Faulds, J.E., Ferrari, L., Grose, T.L.T., Henry, C.D., Janacke, S.U., Miller, D.M., Richard, S.M., Rowley, P.D., Roldán-Quintana, J., Scott, R.B., Sears, J.W., and Williams, V.S., 1998, Map showing Cenozoic tilt domains and associated structural features, western North America, *in* Faulds, J.E., and Stewart, J.H., eds., *Accommodation zones and transfer zones: The regional segmentation of the Basin and Range province: Geological Society of America Special Paper 323*, Plate 1.
- Sun, M.-S., and Baldwin, B., 1958, Volcanic rocks of the Cienega area, Santa Fe County, New Mexico: *New Mexico Bureau of Mines and Mineral Resources Bulletin 54*, 80 p.
- Tedford, R.H., and Barghoorn, S., 1999, Santa Fe Group (Neogene), Ceja del Rio Puerco, northwestern Albuquerque basin, Sandoval County, New Mexico, *in* Pazzaglia, F.J., et al., eds., *Albuquerque geology: New Mexico Geological Society, 50th Field Conference, Guidebook*, p. 327–336.
- U.S. Geological Survey, Sander Geophysics Ltd., and Geoterra-Digham, 1999, Digital aeromagnetic data from the Sandoval, Santa Fe, Belen, and Cochiti airborne surveys: U.S. Geological Survey Open-File Report 99–104, 1 compact disc.

MANUSCRIPT RECEIVED BY THE SOCIETY NOVEMBER 19, 1999
 REVISED MANUSCRIPT RECEIVED JUNE 5, 2000
 MANUSCRIPT ACCEPTED JUNE 30, 2000

Printed in the USA